



## Impact of standardization in tissue processing: the performance of different fixatives

Eleonora De Martino<sup>a</sup>, Caterina Medeot<sup>a</sup>, Lorenzo D'Amico<sup>b,c</sup>, Giorgio Stanta<sup>a</sup>, Serena Bonin<sup>a,\*</sup>

<sup>a</sup> Department of Medical Sciences, University of Trieste, Trieste, Italy

<sup>b</sup> Department of Physics, University of Trieste, Trieste, Italy

<sup>c</sup> Elettra-Sincrotrone Trieste S.C.p.A., Area Science Park, Trieste, Italy

### ARTICLE INFO

#### Keywords:

ISO standard  
Pre-analytical processes  
Formalin  
Bouin  
Paraffin embedding

### ABSTRACT

Most tissues in clinical practice are formalin-fixed and paraffin-embedded for histological as well as molecular analyses. The reproducibility and uniformity of molecular analyses is strictly dependent on the quality of the biomolecules, which is highly influenced by pre-analytical processes. In this study, the effect of different fixatives was compared, including formalin, Bouin's solution, RCL2® and TAG-1™ fixatives, by stringent application of ISO standards in mouse liver tissue processing, including formalin-free transport of tissues and tissue grossing in a refrigerated environment. The effect of fixatives was studied in terms of nucleic acid quality at the time of tissue processing and after one year of tissue storage at room temperature in the dark. Furthermore, a microcomputed tomography (CT) scan analysis was applied to investigate the paraffin embedding. The results show that the application of ISO standards in tissue processing allows analysis of 400 bases amplicons from RNA and 1000 bases from DNA, even in extracts from formalin-fixed and paraffin-embedded tissues. However, after one year storage at room temperature in the dark, a degradation of the nucleic acids was observed. Nevertheless, extracts can still be analyzed, but for metachronous tests it is highly recommended to repeat the quantitation of housekeeping genes in order to standardize the extent of nucleic acid degradation.

### 1. Introduction

The standardization of pre-analytical processes is pivotal both in diagnostic and biomedical research in order to obtain reliable and reproducible results. Increasingly, diagnosis relies on molecular analyses, the reproducibility and uniformity of which depend strictly on the quality of the biomolecules, which is highly influenced by pre-analytical processes [1,2]. Several factors influence biomolecular quality and the following analytical results. For solid tissues, those factors span from specimen collection to data analysis and include warm and cold ischemia, the type of stabilization or fixation, time of fixation, specimen thickness, type of paraffin, the storage conditions and the biomolecule extraction procedures [3]. Fresh unfixed tissues are the gold standard in terms of biomolecule quality, but freezing is far from a routine process in hospitals, where solid tissues from biopsy and surgical procedures are mostly formalin-fixed and paraffin-embedded. Nowadays, through the publication of ISO standards [4–6] focused on pre-analytical processes

for in vitro diagnostics (IVD) analyses from formalin-fixed and paraffin-embedded (FFPE) tissues, the variability range in tissue processing has narrowed. Nevertheless, the application of those international standards in hospitals are not mandatory and, where applied, the extent to which the standard is followed could be variable. ISO standards on tissue transport from the operating theatre allow both formalin-free procedures at 2–8 °C as well as tissue transport in standard buffered formalin at room temperature (RT) [4].

In addition to formalin, other fixatives could be used in parallel for specific purposes, including Bouin's solution, which in the past has been used to analyze morphological details such as in testis biopsies [7]. Because of the high acidic pH, Bouin's fixative is detrimental to nucleic acids and protein analysis [7–9]. Alcohol-based fixatives (such as Fine-FIX and RCL2®) allow a better preservation of both nucleic acids and proteins [10,11]. Recently, TAG-1™ fixative has been introduced to replace formalin [12]. It is a non-crosslinking fixative that has been designed to preserve DNA, RNA and protein quality, with the advantage

*Abbreviations:* BFPE, Bouin's solution-fixed and paraffin-embedded; FF, Fresh frozen; FFPE, Formalin-fixed and paraffin-embedded; ISO, International Organization for Standardization; Micro CT, Microcomputed Tomography; RFPE, RCL2®-fixed and paraffin-embedded; TFPE, TAG-1™-fixed and paraffin-embedded.

\* Correspondence to: DSM-Department of Medical Sciences, Cattinara Hospital, Strada di Fiume 447, Trieste 34149, Italy.

E-mail address: [sbonin@units.it](mailto:sbonin@units.it) (S. Bonin).

<https://doi.org/10.1016/j.nbt.2022.07.001>

Received 15 March 2022; Received in revised form 21 July 2022; Accepted 21 July 2022

Available online 22 July 2022

1871-6784/© 2022 Published by Elsevier B.V. This is an open access article under the CC BY-NC-ND license (<http://creativecommons.org/licenses/by-nc-nd/4.0/>).

of using for immunohistochemistry the same protocols applied to FFPE tissues.

In this study, the effect of different fixatives, including formalin, Bouin's solution, RCL2® and TAG-1™, was compared in stringent application of ISO standards in mouse liver tissue processing, including formalin-free tissue transport and tissue grossing in a refrigerated environment. The effect of fixatives was studied in terms of nucleic acids quality at the time of tissue processing (January 2020) and after 18 months of tissue storage at RT in the dark (July 2021).

## 2. Material and methods

### 2.1. Specimens

#### 2.1.1. Tissue collection

Liver tissues were harvested post-mortem from 12 Black Swiss mice at the ICGEB animal house in Trieste, Italy. Livers were washed in phosphate buffered saline (PBS), dried on paper and immediately placed on dry ice for transport. In the histopathology institute, livers were sampled at 4 °C using a cutting board on wet ice and submitted to different fixation solution, namely formalin, Bouin's solution (Cat. No. HT10132, Sigma-Aldrich, Saint Louis, MO, USA), RCL2® (Alphelys, Plaisir, France) and TAG-1™ (Truckee Applied Genomics LLC, Reno, NV, USA) for 24 h in the dark at RT. Triplicates were processed for each fixative. Each liver tissue was subdivided in order to have an equal representation in triplicates of all fixatives. Subsequently, fixed samples were washed with PBS, dehydrated and paraffin-embedded following standard procedures. Dehydration was carried out as follows: 5 min EtOH (Cat. No. 32205, Sigma-Aldrich) 50 % (tap water), 10 min EtOH 50 % (tap water), 1 h EtOH 50 % (tap water); 3x in EtOH 75 %, notably 2x for 30 min and the third time for 10 min; 3x in EtOH 80 % as described for EtOH 75 % and 3x in EtOH 95 % as described for EtOH 75 % and 2x in absolute EtOH for 30 min each. Clarification was carried out with xylene (Cat. No. 247642, Sigma-Aldrich), 2x for 30 min. Paraffin embedding was carried out following ISO standard [4]. Fixed and embedded specimens were stored in the dark at RT for one year.

#### 2.1.2. Fresh frozen tissues

Each replicate was powdered in a mortar and pestle with liquid nitrogen in dry ice to avoid tissue thawing. Tissue powder was divided into 4 aliquots, weighed and immediately stored at –80 °C or processed for total RNA and DNA isolation.

### 2.2. Biomolecule extraction

#### 2.2.1. RNA extraction from fresh frozen samples

Fresh frozen tissues were processed using the Maxwell® RSC miRNA tissue kit (Cat. No. AS1460; Promega, Madison WI, USA). Briefly, on average, 74 mg of fresh frozen tissue powder was homogenized with 400 µl of 1-thioglycerol/homogenization solution, 400 µl of Lysis Buffer, 30 µl of proteinase K and incubated at RT for 10 min using manufacturer's instructions. The lysate volume was transferred into two Maxwell® RSC cartridges and total RNA was automatically eluted in 50 µl of nuclease-free water using the Maxwell® RSC instrument (Promega). Samples were divided into aliquots and stored at –80 °C.

#### 2.2.2. RNA extraction from fixed and embedded tissues

Total RNA was isolated from four 10 µm-thick sections of fixed and paraffin embedded tissues using the Maxwell® RSC instrument as previously reported [13]. Briefly, sections were de-waxed with mineral oil, digested with 25 µl of proteinase K, de-crosslinked and treated with DNase I (Promega) with the Maxwell® RSC RNA FFPE kit (Cat. No. AS1440; Promega) using manufacturer's instructions. Successively, the 1-thioglycerol/homogenization solution and lysis buffer (MC501C) were added to the aqueous phase. The lysate volume was transferred to the Maxwell® RSC cartridge (Cat. No. AS1460; Promega) and

automatically eluted in 50 µl of Nuclease-free water. RNA concentration and purity were checked through NanoDrop™ ND-1000 spectrophotometer (Thermo Fischer Scientific, Waltham MA, USA). The 260/280 absorption ratio was used to assess the purity of nucleic acids. A ratio of 2.0 was considered as “pure” for RNA; lower values may indicate the presence of protein, phenol or other contaminants. Samples were divided into aliquots and stored at –80 °C.

#### 2.2.3. DNA extraction from fresh frozen tissues

DNA was isolated using Maxwell® RSC instrument from 93 mg (fresh frozen sample 1), 20 mg (fresh frozen sample 2) and 89 mg (fresh frozen sample 3) of tissue powder. 30 µl of proteinase K (Promega) and 300 µl of Lysis Buffer (Promega) were mixed with a maximum amount of 40 mg of sample and incubated at 56 °C for 20 min. In case of higher tissue amounts, parallel isolations were performed. Each lysate was transferred to a Maxwell® RSC Blood DNA cartridge (Cat. No. AS1400; Promega). DNA was eluted in 50 µl of Elution Buffer provided by the Maxwell® RSC Blood DNA kit (Cat. No. AS1400; Promega), divided into aliquots and stored at –80 °C. DNA concentration and purity were measured by NanoDrop™ ND-1000 spectrophotometer (Thermo Fisher Scientific). The 260/280 absorption ratio was used to assess the purity of nucleic acids. A ratio of 1.8 was considered as “pure” for DNA; lower values may indicate the presence of protein, phenol or other contaminants.

#### 2.2.4. DNA extraction from fixed and embedded tissues

Two 10 µm-thick tissue sections were collected into a 1.5 ml sterile microcentrifuge tube (Sarstedt AG & Co. KG, Nümbrecht, Germany) and DNA was extracted using Maxwell® RSC instrument according to the manufacturer's instructions (Cat. No. AS1450; Promega). The sections were de-waxed in 300 µl of mineral oil and digested with Lysis Buffer solution at 56 °C for 30 min, then at 80 °C for 4 h. After the digestion and RNase A (Promega) treatment, DNA was eluted in 50 µl of nuclease free water and its concentration and purity were checked through NanoDrop™ ND-1000 spectrophotometer. Samples were divided and stored at –80 °C until use.

### 2.3. RNA analysis

#### 2.3.1. RNA integrity

RNA integrity was investigated through automated electrophoresis using the Agilent 2100 Bioanalyzer instrument (Agilent Technologies, Santa Clara, CA, USA). 1 µl of each sample was loaded into a well of the Agilent RNA 6000 Nano Chip (Cat. No. 5067–1529; Agilent Technologies) which was previously filled with gel-dye mixture and 5 µl of RNA 6000 Nano Marker, as described in the manufacturer's instruction (Cat. No. 5067–1512; Agilent Technologies). In addition, the distribution of different length fragments was measured by the relative abundance in comparison with the total RNA area. Five ranges were defined as follows: from 1 to 59 nucleotides (1), 60–149 (2), 150–299 (3), 300–449 (4) and 450–600 (5).

#### 2.3.2. DNase I treatment

50 µl and 30 µl of total RNA from FF and fixed and embedded tissues were treated with 30 U of DNase I (Cat. No. 04716728001; Roche, Mannheim, Germany) and 20 U of RNase Inhibitor (Cat. No. N8080119; Thermo Fisher Scientific) at 25 °C for 20 min, then the reaction was stopped with 4 µl of EDTA 25 mM at 65 °C for 10 min [14]. Samples were divided into aliquots and stored at –80 °C.

#### 2.3.3. Reverse transcription and real-time PCR assay

1 µg of total RNA was reverse transcribed into cDNA using 6 µg of hexamers (IDT- Integrated DNA Technologies, Inc., Coralville, IA, USA), 250 U of M-MLV reverse transcriptase (Cat. No. 28025013; Thermo Fisher Scientific), 1 mM dNTPs (Cat. No. U1330, Promega), 0.01 M DTT (ThermoFisher Scientific), 4.5 mM MgCl<sub>2</sub> (ThermoFisher Scientific) and 8 U RNase Inhibitors (Cat. No. N8080119; ThermoFisher Scientific) as

previously reported [15].

Three genes with different expression levels were analyzed: *mt-CO1* (cytochrome c oxidase I, mitochondrial) was studied for its stability and resistance to ribonuclease degradation; *GAPDH* (glyceraldehyde-3-phosphate dehydrogenase) because of its high expression, and in contrast *HPRT* (hypoxanthine phosphoribosyltransferase 1) for its low expression.

For quantitative real-time PCR, 25 ng of cDNA was mixed with Fast EvaGreen® qPCR Master Mix 2X (Cat. No. 31003; Biotium, Fremont, CA, USA), and 300 nM of reverse and forward primers (IDT, USA) as reported in Table 1 in a final volume of 20 µl. Each reaction was carried out in duplicate on a CFX96 Touch Real Time PCR Detection system (Biorad, Hercules, CA, USA) using the following cycling conditions: 2 min at 95 °C, 45 cycles at 95 °C for 20 s, appropriate annealing temperature for 30 s and the extension at 72 °C for 30 or 60 s. Melting curve analysis was performed to evaluate the amplification specificity. A fourth step for fluorescence reading was added to analyze *HPRT* 223 bp and 395 bp amplicons (1 min at 77 °C or 78 °C, respectively). *HPRT* 140 and 184 bp length was amplified only for Bouin's fixed and embedded samples because of their extensive degradation.

## 2.4. DNA analysis

### 2.4.1. Real-time PCR assay

To analyze DNA integrity, the *HPRT* amplicons of 60 (short, S), 223 (medium, M) and 1062 (long, L) bp length were amplified by real time PCR.

25 ng of DNA were amplified with Fast EvaGreen® qPCR Master Mix 2X (Biotium), 300 nM of reverse and forward primers (IDT) (Table 2) in a final volume of 20 µl. Each reaction was carried out in duplicate on a Mastercycler® ep Realplex (Eppendorf, Hamburg, Germany) using the following cycling conditions: 2 min at 95 °C, 45 cycles at 95 °C for 20 s, appropriate annealing temperature for 30 s and the extension at 72 °C for 30 or 60 s; the melting curve was performed to evaluate amplification specificity (Table 2). A fourth step for fluorescence reading was added to analyze *HPRT* 223 bp and 1062 bp amplification (1 min at 77 °C or 78 °C, respectively).

**Table 1**

Primers and amplification conditions for *GAPDH*, *HPRT* and *mt-CO1* analysis.

Gene name	Size bp	Primer sequence	Annealing Temp.	Extension Temp.	
<i>Mus-musculus mt-CO1</i> [33]	60	Forward	5'-CAGTTGGTGGTCTAACCCGGAATTGT-3'	60 °C/30''	72 °C/30''
	(S short)	Reverse	5'-CGTGAAGCACGATGTCAAGGGA-3'		
	179	Forward	5'-CAGTTGGTGGTCTAACCCGGAATTGT-3'	57.5 °C/30''	72 °C/30''
	(M medium)	Reverse	5'-TGTGTCATCTAGGGTGAAGCCTGA-3'		
<i>Mus-musculus GAPDH</i>	302	Forward	5'-CAGTTGGTGGTCTAACCCGGAATTGT-3'	61 °C/30''	72 °C/45''
	(L long)	Reverse	5'-TGTGGTGAAGCATCTGGGTAGTCT-3'		
	90	Forward	5'-ATGGTGAAGGTCGGTGTGAA-3'	60 °C/30''	72 °C/30''
	(S short)	Reverse	5'-GGCAACAATCTCCACTTTGC-3'		
<i>Mus-musculus HPRT</i>	185	Forward	5'-AGACAAAATGGTGAAGGTCGG-3'	60 °C/30''	72 °C/45''
	(M medium)	Reverse	5'-CCTTGACTGTGCCGTTGAAT-3'		
	267	Forward	5'-CAAATGGTGAAGGTCGGTGT-3'	60 °C/30''	72 °C/1'
	(L long)	Reverse	5'-GCCTCACCCCATTTGATGTT-3'		
<i>Mus-musculus HPRT</i>	60	Forward	5'-CTGCGTCCCCAGACTTTGA-3'	57 °C/30''	72 °C/30''
	(S short)	Reverse	5'-TCTACCAGAGGTTAGGCTGG-3'		
	140 ‡	Forward	5'-CTGTGGCCATCTGCCTAGTA-3'	59 °C/30''	72 °C/45''
	(M medium)	Reverse	5'-TCTACCAGAGGTTAGGCTGG-3'		
	184 ‡	Forward	5'-GAGTCCTGTTGATGTTGCCAGT-3'	59 °C/30''	72 °C/45''
	(L long)	Reverse	5'-TCTACCAGAGGTTAGGCTGG-3'		
	223 *	Forward	5'-CTGTGGCCATCTGCCTAGTA-3'	59 °C/30''	72 °C/1'
	(M medium)	Reverse	5'-TCCTTCTACAGATACAATCTCAGT-3'		
	395 #	Forward	5'-TGTTGTTGGATATGCCCTTGAC-3'	58 °C/30''	72 °C/1'
	(L long)	Reverse	5'-TCCTTCTACAGATACAATCTCAGT-3'		

\* Fluorescence reading step at 77 °C for 1 min

# Fluorescence reading step at 78 °C for 1 min

‡ Amplicon length used only for BFPE samples

## 2.5. Real time PCR efficiency

To evaluate real time PCR efficiency, standard curve analyses was carried out on a pool of extracts made in years 2020 and 2021 for all genes. Pools of 2020 and 2021 were generated mixing DNA or cDNA from all fixed and embedded samples, after which two-fold serial dilution was amplified. 100 ng, 50 ng, 25 ng, 12.5 ng and 6.25 ng of DNA and 50 ng, 25 ng, 12.5 ng, 6.25 and 3.12 ng of cDNA were mixed with the amplification solution as reported in the previous paragraph. The amplification was performed in duplicate on a CFX96 Touch Real Time PCR Detection system (Biorad) following the above-mentioned cycling conditions.

## 2.6. Microcomputed tomography (Micro-CT) of fixed and paraffin-embedded samples

The micro-CT scans were performed at SYRMEP beamline of the Elettra synchrotron light (Trieste, Italy). Samples were measured in propagation based phase contrast modality with a sample-to-detector distance of 50 cm. The polychromatic beam was filtered with 1 mm of silica resulting in a mean X-Ray energy of 20 keV. The detector was an Orca Flash SCMOS (Hamamatsu Photonics Italy SRL, Milan, Italy) coupled with a 45 µm thickness GGG scintillator. The scans were performed over 180° for a total of 1800 projection with an exposure time of 100 ms. The pixel size was set to 4 µm resulting in a field of view of 8 mm x 8 mm. The reconstructions were performed using the beamline custom made software STP (SYRMEP Tomo Project) [16]. A phase retrieval algorithm [17] was applied before the use of the conventional filtered back projection algorithm in order to increase the image contrast, with the  $\delta/\beta$  set to 100.

## 2.7. Statistical Analysis

Data distribution was investigated by Shapiro-Wilk test. Parametric or non-parametric tests were applied for statistical analysis according to data distribution. Paired t-test and Wilcoxon matched-pairs signed rank test were run to investigate nucleic acid purity and integrity. To compare the efficiency between the 2020 and 2021 real time PCR amplifications, the Ancova test was applied.

**Table 2**  
Primer sequences and amplification conditions for DNA analysis.

Gene name	Size bp	Primer sequence	Annealing Temp.	Extension Temp.	
<i>Mus-musculus</i> <i>HPRT</i>	60 (S short)	Forward	5'-CTGCGTCCCAGACTTTTGA-3'	57 °C/30''	72 °C/30''
		Reverse	5'-TCTACCAGAGGGTAGGCTGG-3'		
	223 * (M medium)	Forward	5'-CTGTGGCCATCTGCCTAGTA-3'	59 °C/30''	72 °C/1'
		Reverse	5'-TCCTTCTTACAGATACAATCTCAGT-3'		
	1062 # (L long)	Forward	5'-TGTTGTTGGATATGCCCTTGAC-3'	58 °C/30''	72 °C/2'
		Reverse	5'-TCCTTCTTACAGATACAATCTCAGT-3'		

\* Fluorescence reading step at 77 °C for 1 min

# Fluorescence reading step at 78 °C for 2 min

For each pre-analytical condition, mouse livers were processed in triplicate. The results are reported as the average value of triplicates.

All the statistical analyses were carried out using the GraphPad Prism 8.0 software (San Diego, CA, USA).

### 3. Results

#### 3.1. Nucleic acid yields and purity

The nanodrop method was applied to quantify total nucleic acid yield and purity, which were similar in extracts obtained in 2020 and 2021 (see [Supplementary Fig. S1](#)).

Total RNA purity was measured by A260/280 and A260/230 ratios. The average A260/280 ratio was 2.02 (1.9–2.1) and no differences were found between measurements made in 2020 and 2021 ( $p = 0.5$ , see [supplementary Fig. S2a](#)). The average A260/230 ratio was 1.94 (1.4–2.2) and the lowest value was detected in FF samples with an average of 1.8 (1.7–1.9). ([Supplementary Fig. S2b](#)). By stratifying data per fixative, ratios measured in 2021 resulted lower than those made in 2020, for Bouin's solution-fixed and paraffin-embedded (BFPE) and RCL2®- fixed and paraffin-embedded (RFPE) samples ( $p$  values 0.0008 and 0.03, respectively).

For DNA the mean A260/280 value was 1.9 (1.5–2.0) and the Bouin's fixed mouse liver had the lowest ratio value ( $p = 0.0005$ ) ([Supplementary Fig. S2c](#)). Lower ratio values were measured in 2021, namely in formalin, RCL2® and TAG-1™ fixed and embedded samples ( $p = 0.04$ ,  $p = 0.01$  and  $p = 0.03$ , respectively). The mean A260/230 ratio was 1.6 (0.7–1.9) with relevant variability among samples, BFPE samples in particular had the lowest values. In addition, the FFPE and RFPE samples had significant lower ratio values in 2021 than 2020 measurements ( $p = 0.04$  and  $p = 0.01$ , respectively) ([Supplementary Fig. S2d](#)).

#### 3.2. Nucleic acids integrity

RNA Integrity (RIN) was investigated by Agilent 2100 Bioanalyzer by RIN metric and fragments analysis. On average the RIN number was 2.4 (2.2–2.9) for fixed and embedded livers analyzed in 2020 and 2.3

**Table 3**

Results of the Agilent 2100 Bioanalyzer analysis. The average RIN values obtained from mouse livers treated with different pre-analytical conditions are reported. The p-value refers to Wilcoxon matched-pairs signed rank test. FFPE: Formalin fixed and paraffin embedded; BFPE: Bouin's fixed and paraffin embedded; RFPE: RCL2® fixed and paraffin embedded; TFPE: TAG-1™ fixed and paraffin embedded; FF: Fresh Frozen samples.

Sample name	RIN 2020	RIN 2021	$p$ value <sup>1</sup>
FFPE	2.5 (2.3–2.9)	2.1 (2.0–2.4)	0.4
BFPE	2.5 (2.5–2.5)	2.3 (1.9–2.3)	
RFPE	2.4 (2.3–2.4)	2.4 (2.0–2.6)	
TFPE	2.3 (2.2–2.3)	2.5 (2.2–2.6)	
FF	6.4 (6.2–6.5)		

<sup>1</sup>  $p$  value refers to Wilcoxon matched-pairs signed rank test

(1.9–2.6) for measurements in 2021, while it was 6.4 (6.2–6.5) for FF samples ([Table 3](#)). No significant difference was detected for RIN values in fixed and embedded samples ( $p = 0.4$ ) ([Table 3](#)).

Fragment analysis has highlighted the 150–299 fraction as the most representative in almost all fixed and embedded samples (mean value 19 %), as shown in [supplementary Fig. S3](#). No significant differences were detected in fragment analysis between RNA extracts processed in 2020 and 2021 ([Supplementary Fig. S3](#)).

#### 3.3. Real Time PCR efficiency

Standard curve equations from linear regression analysis are reported in [supplementary Table S1](#). Significant differences were found for small amplicons of the *HPRT* gene, both for mRNA and DNA sequences ( $p = 0.03$  and  $p = 0.003$ , respectively). Overall, biomolecule amplification in the two years does not seem to be influenced by inhibitory factors.

#### 3.4. Biomolecule analysis

To analyze the effects of storage among fixatives, *mt-CO1*, *GAPDH* and *HPRT* gene expression was analyzed by real time PCR. As reported in material and methods section, three amplicon lengths were amplified for *mt-CO1* (60, 179 and 302 bp), *GAPDH* (90, 185 and 267 bp) and *HPRT* (60, 223 and 395 bp). For Bouin's fixed and embedded samples, because of their degradation, only the 60, 140 and 184 bp amplicons of *HPRT* were analyzed ([supplementary Table S2](#)).

Long sequences (up to 395 bp) of all genes were amplified in all fixatives, with some exceptions; namely the longest *GAPDH* (267 bp) fragment was not amplified from RNA samples obtained from BFPE tissues, in both the 2020 and 2021 analyses. Furthermore, no amplification resulted for the longest *HPRT* sequence (395 bp) in the 2021 extracts from TAG-1™ fixed mouse liver ([Table 4](#)).

Degradation kinetics were evaluated comparing the threshold cycles (Ct) obtained in 2020 and 2021 analyses; specifically, the Ct increment of long amplicons reflects the degradation of long RNA stretches during storage ([Table 4](#)). Generally, after 18 months of storage, Ct values increased in all fixed and embedded samples for all analyzed genes. The effect of storage on the analyzed fixatives was highlighted for the *HPRT* gene, where on average a difference of 6 Cts was recorded between analyses carried out in 2020 and 2021 for the longest sequence ( $p < 0.0001$ ). Similar results were obtained for the longest amplicon of *GAPDH* where a deviation of 3.5 Ct between the determinations made in the two years was detected ( $p = 0.0003$ ). In contrast, no significant differences were found in the analysis of *mt-CO1*, except for formalin fixed and embedded samples where a difference of 1 Ct was detected in all amplicon lengths ([Table 4](#)).

Similarly for DNA, three amplicon lengths of *HPRT* were amplified to investigate DNA integrity after mid-term storage. The longest *HPRT* sequence (1062 bp) was amplified in all fixed and embedded samples, except for DNA extracted from BFPE tissue. Therefore, for Bouin's fixed and embedded samples, only the Ct of 60 bp amplification was reported in [Table 4](#) because for those specimens, amplicons longer than 184 bp

**Table 4**

Results of biomolecule amplifications. Mean threshold cycle (Ct)  $\pm$  SD of long (L), medium (M) and short (S) amplicon of *mt-CO1*, *GAPDH* and *HPRT* genes for mRNA and *HPRT* for DNA analysis are reported. FFPE: Formalin fixed and paraffin embedded; BFPE: Bouin's fixed and paraffin embedded; RFPE: RCL2<sup>®</sup> fixed and paraffin embedded; TFPE: TAG-1<sup>™</sup> fixed and paraffin embedded; FF: Fresh Frozen samples; ND: non-detectable. <sup>1</sup>The p-value refers to paired t-test.

Biomolecule	Gene	Fixative	Ct L 2020	Ct L 2021	p value <sup>1</sup>	p value <sup>1</sup>	Ct M 2020	Ct M 2021	p value <sup>1</sup>	p value <sup>1</sup>	Ct S 2020	Ct S 2021	p value <sup>1</sup>	p value <sup>1</sup>
mRNA	<i>Mus-musculus mt-CO1</i>	FFPE	25.4 $\pm$ 0.6	26.6 $\pm$ 0.6	0.0008	0.02	17.6 $\pm$ 0.6	18.3 $\pm$ 0.4	0.01	0.04	17.6 $\pm$ 0.4	16.2 $\pm$ 0.3	0.004	0.0003
		BFPE	33.9 $\pm$ 1.6	34.6 $\pm$ 0.4	0.4		25.9 $\pm$ 2.1	27.3 $\pm$ 1.4	0.1		21.5 $\pm$ 0.7	20.0 $\pm$ 0.7	0.0007	
		RFPE	23.4 $\pm$ 1.0	24.6 $\pm$ 0.3	0.1		17.5 $\pm$ 1.0	17.2 $\pm$ 0.2	0.6		17.9 $\pm$ 0.9	16.0 $\pm$ 0.08	0.05	
		TFPE	27.2 $\pm$ 0.4	27.8 $\pm$ 0.5	0.2		19.7 $\pm$ 0.2	20.3 $\pm$ 0.7	0.4		18.4 $\pm$ 0.3	18.1 $\pm$ 0.6	0.6	
		FF	24.8 $\pm$ 1.2				17.7 $\pm$ 0.7				17.3 $\pm$ 0.5			
		FFPE	29.4 $\pm$ 0.4	32.6 $\pm$ 0.6	0.001	0.0003	22.8 $\pm$ 0.3	24.2 $\pm$ 0.3	0.003	0.04	20.3 $\pm$ 0.3	24.1 $\pm$ 0.2	0.0003	< 0.0001
	<i>Mus-musculus GAPDH</i>	BFPE	ND	ND			34.0 $\pm$ 2.1	35.0 $\pm$ 0.8	0.5		27.3 $\pm$ 1.2	28.9 $\pm$ 0.8	0.02	
		RFPE	29.8 $\pm$ 0.9	31.6 $\pm$ 0.6	0.05		24.3 $\pm$ 0.8	23.6 $\pm$ 0.3	0.2		22.0 $\pm$ 0.6	23.9 $\pm$ 0.1	0.02	
		TFPE	30.9 $\pm$ 0.4	36.3 $\pm$ 0.6	0.01		25.3 $\pm$ 0.6	27.7 $\pm$ 0.3	0.04		22.3 $\pm$ 0.4	26.7 $\pm$ 0.3	0.007	
		FF	27.0 $\pm$ 0.5				22.1 $\pm$ 0.5				20.5 $\pm$ 0.4			
		FFPE	33.7 $\pm$ 0.7	41.1 $\pm$ 0.8	0.01	< 0.0001	30.1 $\pm$ 0.6	34.6 $\pm$ 0.4	0.001	0.2	26.3 $\pm$ 0.3	27.3 $\pm$ 0.3	0.007	0.009
		BFPE	ND	ND			ND	ND			30.6 $\pm$ 0.7	31.6 $\pm$ 0.6	0.005	
	<i>Mus-musculus HPRT</i>	RFPE	35.0 $\pm$ 1.3	41.3 $\pm$ 0.7	0.02		31.3 $\pm$ 1.3	34.6 $\pm$ 0.3	0.03		27.6 $\pm$ 0.8	27.4 $\pm$ 0.2	0.6	
		TFPE	37.0 $\pm$ 0.4	ND			33.4 $\pm$ 0.2	41.3 $\pm$ 0.9	0.008		28.8 $\pm$ 0.3	31.8 $\pm$ 0.5	0.02	
		FF	33.4 $\pm$ 1.8				33.6 $\pm$ 1.3				26.5 $\pm$ 0.4			
		FFPE	33.4 $\pm$ 0.2	39.2 $\pm$ 1.7	0.02	0.0002	26.1 $\pm$ 0.5	28.2 $\pm$ 0.8	0.04	< 0.0001	25.4 $\pm$ 0.5	25.3 $\pm$ 0.7	0.9	0.3
		BFPE	ND	ND			ND	ND			33.5 $\pm$ 0.6	35.4 $\pm$ 0.8	0.09	
		RFPE	31.7 $\pm$ 2.1	38.1 $\pm$ 1.2	0.05		26.4 $\pm$ 0.6	29.5 $\pm$ 0.6	0.01		25.6 $\pm$ 0.4	25.5 $\pm$ 0.5	0.6	
DNA	<i>Mus-musculus HPRT</i>	TFPE	29.7 $\pm$ 1.2	32.6 $\pm$ 1.4	0.04		25.2 $\pm$ 0.5	26.5 $\pm$ 0.7	0.01		24.8 $\pm$ 0.3	24.4 $\pm$ 0.6	0.1	
		FF	27.2 $\pm$ 0.8				25.7 $\pm$ 0.6				25.9 $\pm$ 0.7			

could not be amplified. Among all fixatives, lower threshold cycles were recorded for DNA isolated from TAG-1<sup>™</sup> samples for all amplicon lengths. Extracts from formalin as well as RCL2<sup>®</sup> fixed and embedded livers had similar Ct measures in both years.

In all fixed and embedded samples the threshold cycle values were higher in 2021 measures than those made in 2020, as shown in Table 4. This difference was specifically magnified in Ct values of long sequences, where on average a difference of 5 Ct was detected between

determinations made in the two reference years ( $p = 0.0002$ ). In contrast, the amplification of short *HPRT* sequences returned the same Ct values in both years for all fixed and embedded samples ( $p = 0.3$ ), except for BFPE sample where a difference of 2 Ct was recorded ( $p = 0.09$ ).

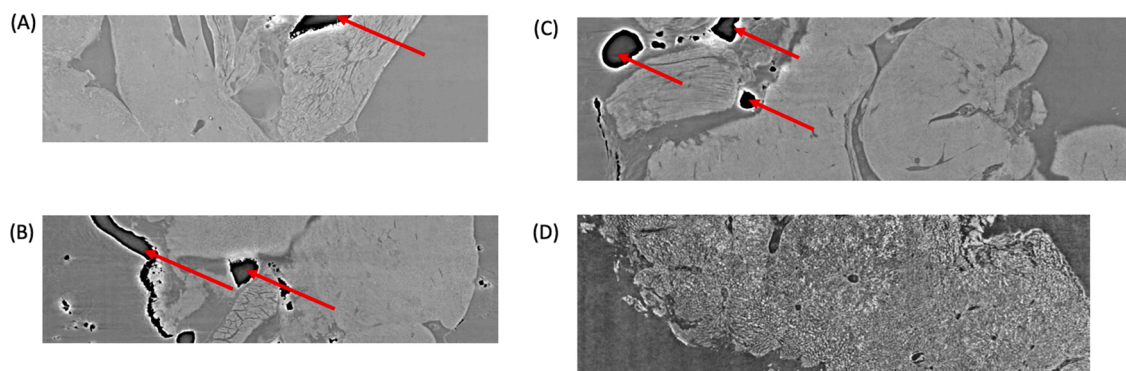


**Fig. 1.** Representative micro CT scan slices from (A) BFPE, (B) FFPE, (C) RFPE and (D) TFPE mouse liver. Arrows indicate the air bubbles.

### 3.5. Micro-CT scans results

In order to inspect the paraffin inclusion, micro-CT scanning was carried out on one representative block for each fixative as shown in Fig. 1. The detection of air bubbles varied with fixative: inclusion for RCL2® resulted in the highest amount of air inside the tissue, followed by formalin, Bouin's solution and TAG-1™ for which only small bubbles were detected outside the tissue. Air bubbles inside the tissue prevent paraffin from segregating. Overall, the results show that paraffin inclusion is not homogeneous and can vary with fixatives.

## 4. Discussion

In this study, mouse livers were processed using different fixative by the application of stringent ISO standards for the pre-analytical processes for RNA analysis from FFPE samples for in vitro diagnostics, in order to investigate the quality of nucleic acids due to fixatives (at the time of tissue processing) and after mid-term storage. The application of the ISO standard allowed amplification of 395 base amplicons of low expression housekeeping gene (*HPRT*) from RNA obtained from non-crosslinking fixatives as well as from formalin. In routine FFPE tissues the amplification of RNA fragments of around 400 bases is far from usual [18], but following strictly the ISO standard with tissue transport in wet ice and tissue sectioning on refrigerated cutting board, it was possible to analyze 400-base RNA stretches even from FFPE specimens. This result is most likely due to the reduction of RNase activity during tissue processing. It is well known that RNases are ubiquitous resistant enzymes [19], so that slowing their activity by temperature decrease allows RT-qPCR results in FFPE livers comparable to those obtained from coagulant fixatives. In agreement with this hypothesis, similar results were reported in RNA extracts from cold formalin fixation and tissue transport under vacuum [20]. In the present study only RNA from BFPE samples did not allow analysis of long stretches of *GAPDH* and *HPRT* genes, but it was possible to amplify even 300 bases of *mt-CO1* gene. The latter result is more likely due to the nature of *mt-CO1*, which is a mitochondrial RNA. Mitochondrial RNAs are transcribed as large, polycistronic precursors, which undergo post-transcriptional processes to liberate functional RNAs, including mRNAs [21]. Mitochondrial mRNA expression is mostly related to their half-lives [21], and *mt-CO1* has one of the longest among mt-mRNAs [22]. Thus, it is likely that the detection of 300 base amplicon of this RNA in BFPE liver is due to its high stability and nature. Threshold values for long amplicons of *HPRT* and *GAPDH* are highly variable among fixatives and, except for Bouin's solution, there was no marked prevalence of one specific fixative. The main difference in the performance of RT-qPCR was mainly based on the expression level of the different genes with higher threshold values of *HPRT* vs *GAPDH*.

The application of the stringent ISO standard for RNA processing also allowed analysis of 1000 bp DNA from all fixed and embedded tissues, except BFPE, DNA from which was highly degraded with only 184 bp amplicons were amplified with Ct values over 35. This result was mainly due to the acidic pH of Bouin's solution and the instability of DNA N-glycosidic bonds resulting in degradation by de-amination [23]. It is well known indeed that DNA depurination is fastened under lower pH conditions [24], as observed in Bouin's solution. The strongly acidic pH of this fixative [9] acts almost immediately due to the fast penetration of acetic acid among the other components [8]. These results are in agreement with other studies reporting that DNA stretches longer than 150 bases are barely amplified from BFPE samples [7]. Although the application of ISO standards allowed a better preservation of nucleic acids at the time of tissue processing, it does not prevent nucleic acid degradation during mid-time storage (18 months) in the archive at RT in dark. An increment in Ct values was observed for *GAPDH* and *HPRT* for most fixatives and amplicon length. By careful observation of mRNA data, TAG-1™ fixed and embedded RNA resulted in the highest difference in Ct between measurements made after 18 months storage. This

could be related to the composition of the fixative, but it was not possible to test this hypothesis as it is patent protected. Nevertheless, DNA from the same fixative resulted in the lowest threshold cycles for the analysis of long as well as medium and short stretches of *HPRT*, even after one year storage, resulting in a better preservation of DNA.

The degradation of nucleic acids in fixed and paraffin embedded tissues during long term storage has already been documented [25–27], but the mechanism describing this degradation continues to be unknown. The present results showed that the fragmentation was detectable for any amplicon length of the *GAPDH* and *HPRT* genes, but with higher sensitivity for the shortest amplicon size, in agreement with others [25,28]. Results of short amplicons of *mt-CO1* are quite intriguing, showing a significant decrease of Ct value after one year. The only explanation is that, after one year, shorter fragments of mt RNA were detected, due to the fragmentation process. Enzymatic degradation of nucleic acids during storage is unlikely as already reported [26], while chemical degradation by oxidation and hydrolysis is the most reasonable mechanism, assuming that traces of water trapped in the tissue due to incomplete processing could play a role [26]. Nevertheless, biomolecular degradation could also be related to embedding procedures. Micro-CT scans of the samples showed, in most samples, an impaired embedding with the presence of air bubbles inside the tissue supporting a non-homogeneous paraffin permeation, as already found in large inclusions [29]. It cannot be excluded that in those microscopic regions fixative-dependent degradation can occur. Up to now degradation due to paraffin embedding was mainly reported to impact on nucleic acids, mostly RNA, at the time of tissue processing due to inclusion temperature and possible RNA aggregation, rather than during storage. However, defective paraffin penetration, which has already been documented in RCL2® fixed and embedded tissues [30], can cooperate with entrapped air in the degradation of macromolecules during storage.

In conclusion, with the exception of Bouin's solution, the actuation of standards for RNA aligns the quality of nucleic acids between formalin and non-crosslinking fixatives, highlighting the necessity to follow stringently these specific ISO documents in hospitals and biobanks. Nevertheless, it is acknowledged that nucleic acids degrade during storage at RT for any fixative. As a consequence, for any analysis requiring the nucleic acid analysis from the same tissue block after years of storage, it is recommended to repeat housekeeping gene analysis in order to standardize the degradation level of nucleic acids.

It is acknowledged that a limitation in this study is that only mouse liver tissue was processed and that other organs/tissues could have different profiles of degradation during tissue processing and/or during storage. It is indeed well known that RNA from pancreas and colon has lower quality mainly due to the high RNase content [31], digestive enzymes and bacterial colonization [32], which impact on RNA degradation during tissue processing. Nevertheless, the results here highlight that formalin free transport of samples reduces nucleic acid degradation, preserving even in formalin long RNA and DNA stretches for molecular investigations [33].

### Declaration of Competing Interest

SB received in January 2020 from Truckee Applied Genomics, LLC, the company producing TAG-1™ fixative, 10 vials with TAG-1 and TAG-2 to test in the laboratory.

### Data Availability

Data will be made available on request.

### Acknowledgements

The authors would like to thank prof. Serena Zacchigna (University of Trieste and ICGEB) and Dr. Willy De Mattia from the ICGEB-

International Centre for Genetic Engineering and Biotechnology of Trieste, for providing the mouse livers for experiments. The authors are grateful to the EU FP7 project SPIDIA (contract no. 222916) and the EU H2020 project SPIDIA4P (contract no. 733112), for the efforts made to create technical documents and standards for pre-analytical conditions for tissue processing useful for in vitro diagnostics. The authors would also thank the EU H2020 project iTBoS (contract no. 965221) which supported the publication of this article.

## Appendix A. Supporting information

Supplementary data associated with this article can be found in the online version at [doi:10.1016/j.nbt.2022.07.001](https://doi.org/10.1016/j.nbt.2022.07.001).

## References

- [1] Bonin S, Stanta G. Pre-analytics and tumor heterogeneity. *N Biotechnol* 2020;55:30–5. <https://doi.org/10.1016/j.nbt.2019.09.007>.
- [2] Dagher G, Becker KF, Bonin S, Foy C, Gelmini S, Kubista M, et al. Pre-analytical processes in medical diagnostics: new regulatory requirements and standards. *N Biotechnol* 2019;52:121–5. <https://doi.org/10.1016/j.nbt.2019.05.002>.
- [3] Compton CC, Robb JA, Anderson MW, Berry AB, Birdsong GG, Bloom KJ, et al. Preanalytics and precision pathology: pathology practices to ensure molecular integrity of cancer patient biospecimens for precision medicine. *Arch Pathol Lab Med* 2019;143:1346–63. <https://doi.org/10.5858/arpa.2019-0009-SA>.
- [4] ISO 20166–1:2018 I. Molecular in vitro diagnostic examinations — Specifications for pre-examination processes for formalin-fixed and paraffin-embedded (FFPE) tissue — Part 1: Isolated RNA. 2018.
- [5] ISO 20166–2:2018 I. Molecular in vitro diagnostic examinations – Specifications for pre-examinations processes for formalin-fixed and paraffin-embedded (FFPE) tissue – Part 2: Isolated proteins. 2018.
- [6] ISO 20166–3:2018 I. Molecular in vitro diagnostic examinations - Specifications for pre-examination processes for formalin-fixed and paraffin-embedded (FFPE) tissue - Part 3: Isolated DNA. 2018.
- [7] Bonin S, Petrerá F, Rosai J, Stanta G. DNA and RNA obtained from Bouin's fixed tissues. *J Clin Pathol* 2005;58:313–6. <https://doi.org/10.1136/jcp.2004.016477>.
- [8] Howat WJ, Wilson BA. Tissue fixation and the effect of molecular fixatives on downstream staining procedures. *Methods* 2014;70:12–9. <https://doi.org/10.1016/j.ymeth.2014.01.022>.
- [9] Fattorini P, Forzato C, Tierno D, De Martino E, Azzalini E, Canzonieri V, et al. A novel HPLC-based method to investigate on RNA after fixation. *Int J Mol Sci* 2020;21:7540.
- [10] Moelans CB, Oostenrijk D, Moons MJ, van Diest PJ. Formaldehyde substitute fixatives: effects on nucleic acid preservation. *J Clin Pathol* 2011;64:960–7. <https://doi.org/10.1136/jclinpath-2011-200152>.
- [11] Dotti I, Bonin S, Basili G, Nardon E, Balani A, Siracusano S, et al. Effects of formalin, methacarn, and FineFIX fixatives on RNA preservation. *Diagn Mol Pathol* 2010;19:112–22. <https://doi.org/10.1097/PDM.0b013e3181b520f8>. ([https://www.pmwintl.com/exhibitor/truckee-applied-genomics-tag\\_2022sv](https://www.pmwintl.com/exhibitor/truckee-applied-genomics-tag_2022sv)).
- [12] De Martino E, Brunetti D, Canzonieri V, Conforti C, Eisendle K, Mazzoleni G, et al. The association of residential altitude on the molecular profile and survival of melanoma: results of an interreg study. *Cancers* 2020;12:2796.
- [13] Dotti I, Bonin S. DNase Treatment of RNA. In: Stanta G, editor. *Guidelines for Molecular Analysis in Archive Tissues*. Berlin, Heidelberg: Springer Berlin Heidelberg; 2011. p. 87–90.
- [14] Nardon E, Donada M, Bonin S, Dotti I, Stanta G. Higher random oligo concentration improves reverse transcription yield of cDNA from bioptic tissues and quantitative RT-PCR reliability. *Exp Mol Pathol* 2009;87:146–51. <https://doi.org/10.1016/j.yexmp.2009.07.005>.
- [15] Brun F, Pacilé S, Accardo A, Kourousias G, Dreossi D, Mancini L, et al. Enhanced and flexible software tools for X-ray computed tomography at the Italian synchrotron radiation facility elettra. *Fundam Inf* 2015;141:233–43. <https://doi.org/10.3233/FI-2015-1273>.
- [16] Paganin D, Mayo SC, Gureyev TE, Miller PR, Wilkins SW. Simultaneous phase and amplitude extraction from a single defocused image of a homogeneous object. *J Microsc* 2002;206:33–40. <https://doi.org/10.1046/j.1365-2818.2002.01010.x>.
- [17] Belloni B, Lambertini C, Nuciforo P, Phillips J, Bruening E, Wong S, et al. Will PAXgene substitute formalin? A morphological and molecular comparative study using a new fixative system. *J Clin Pathol* 2013;66:124–35. <https://doi.org/10.1136/jclinpath-2012-200983>.
- [18] Rait VK, O'Leary TJ, Mason JT. Modeling formalin fixation and antigen retrieval with bovine pancreatic ribonuclease A: I-structural and functional alterations. *Lab Invest* 2004;84:292–9. <https://doi.org/10.1038/labinvest.3700045>.
- [19] Bussolati G, Annaratone L, Medico E, D'Armento G, Sapino A. Formalin fixation at low temperature better preserves nucleic acid integrity. *PLoS One* 2011;6:e21043. <https://doi.org/10.1371/journal.pone.0021043>.
- [20] Kummer E, Ban N. Mechanisms and regulation of protein synthesis in mitochondria. *Nat Rev Mol Cell Biol* 2021;22:307–25. <https://doi.org/10.1038/s41580-021-00332-2>.
- [21] Nagao A, Hino-Shigi N, Suzuki T. Measuring mRNA decay in human mitochondria. *Methods Enzym* 2008;447:489–99. [https://doi.org/10.1016/S0076-6879\(08\)02223-4](https://doi.org/10.1016/S0076-6879(08)02223-4).
- [22] Lindahl T. Instability and decay of the primary structure of DNA. *Nature* 1993;362:709–15. <https://doi.org/10.1038/362709a0>.
- [23] An R, Jia Y, Wan B, Zhang Y, Dong P, Li J, et al. Non-enzymatic depurination of nucleic acids: factors and mechanisms. *PLoS One* 2014;9:e115950. <https://doi.org/10.1371/journal.pone.0115950>.
- [24] Sanchez I, Betsou F, Culot B, Frascaquillo S, McKay SC, Pericleous S, et al. RNA and microRNA stability in PAXgene-fixed paraffin-embedded tissue blocks after seven years' storage. *Am J Clin Pathol* 2018;149:536–47. <https://doi.org/10.1093/ajcp/ajq026>.
- [25] Groelz D, Viertler C, Pabst D, Dettmann N, Zatloukal K. Impact of storage conditions on the quality of nucleic acids in paraffin embedded tissues. *PLoS One* 2018;13:e0203608. <https://doi.org/10.1371/journal.pone.0203608>.
- [26] Guyard A, Boyez A, Pujals A, Robe C, Tran Van Nhieu J, Allory Y, et al. DNA degrades during storage in formalin-fixed and paraffin-embedded tissue blocks. *Virchows Arch* 2017;471:491–500. <https://doi.org/10.1007/s00428-017-2213-0>.
- [27] Antonov J, Goldstein DR, Oberli A, Baltzer A, Pirota M, Fleischmann A, et al. Reliable gene expression measurements from degraded RNA by quantitative real-time PCR depend on short amplicons and a proper normalization. *Lab Invest* 2005;85:1040–50. <https://doi.org/10.1038/labinvest.3700303>.
- [28] Zhanmu O, Yang X, Gong H, Li X. Paraffin-embedding for large volume bio-tissue. *Sci Rep* 2020;10:12639. <https://doi.org/10.1038/s41598-020-68876-5>.
- [29] Masir N, Ghoddoosi M, Mansor S, Abdul-Rahman F, Florence CS, Mohamed-Ismail NA, et al. RCL2, a potential formalin substitute for tissue fixation in routine pathological specimens. *Histopathology* 2012;60:804–15. <https://doi.org/10.1111/j.1365-2559.2011.04127.x>.
- [30] Jun E, Oh J, Lee S, Jun HR, Seo EH, Jang JY, et al. Method optimization for extracting high-quality RNA from the human pancreas tissue. *Transl Oncol* 2018;11:800–7. <https://doi.org/10.1016/j.tranon.2018.04.004>.
- [31] Zeugner S, Mayr T, Zietz C, Aust DE, Baretton GB. RNA quality in fresh-frozen gastrointestinal tumor specimens-experiences from the tumor and healthy tissue bank TU Dresden. *Recent Results Cancer Res* 2015;199:85–93. [https://doi.org/10.1007/978-3-319-13957-9\\_9](https://doi.org/10.1007/978-3-319-13957-9_9).
- [32] Bjoerkman J, Kubista M. Methods for assessing RNA quality. Patent number PCT/EP2013/055832, 2013 info available at: <https://patentscope.wipo.int/search/en/detail.jsf?docId=WO2013139860&tab=PCTDESCRIPTION>.